

System Tests with DC-DC Converters for the CMS Silicon Strip Tracker at SLHC

K. Klein, L. Feld, R. Jussen, W. Karpinski, J. Merz, J. Sammet

for the CMS Tracker Collaboration

1. Physikalisches Institut B, RWTH Aachen University, 52074 Aachen, Germany

katja.klein@cern.ch

Abstract

The delivery of power is considered to be one of the major challenges for the upgrade of the CMS silicon strip tracker for SLHC. The inevitable increase in granularity and complexity of the device is expected to result in a power consumption comparable or even higher than the power consumption of today's strip tracker. However, the space available for cables will remain the same. In addition, a further increase of the tracker material budget due to cables and cooling is considered unacceptable, as the performance of the CMS detector must not be compromised for the upgrade. Novel powering schemes such as serial powering or usage of DC-DC converters have been proposed to solve the problem. To test the second option, substructures of the current CMS silicon strip tracker have been operated for the first time with off-the-shelf DC-DC buck converters as well as with first prototypes of custom-designed DC-DC converters. The tests are described and the results are discussed.

I. INTRODUCTION

A. Power Distribution in the CMS Strip Tracker

The current CMS silicon strip tracker [1] is built of 15 148 silicon strip modules. The power consumption per module including the optical conversion is 1.8 or 2.7 W (depending on the module type); the whole strip tracker consumes about 33 kW. Groups of 2-12 modules are powered in parallel via roughly 50 m long copper low impedance cables from CAEN power supplies that are located on the balconies of the experimental cavern. The voltage drop on these long cables leads to a loss of 34 kW, i.e. 50% of the total delivered power is lost in the cables. The current power system is described in detail in [2]. The power lost inside the cold volume of the tracker contributes to the total heat load, which has to be removed to ensure that the sensors are kept at temperatures below -10°C , as required to avoid thermal runaway effects. Power cables and cooling structures increase the material budget of the tracker considerably. The routing and installation of the services has been one of the most complex tasks during tracker commissioning.

Currently plans for an upgrade of the CMS strip tracker are developed in view of a potential luminosity upgrade of the LHC, the Super-LHC (SLHC). While the design is still under study, it is obvious that the granularity of the tracker will have to be increased, while additional complexity will have to be added; in particular, if the tracker information is to be used in the first level trigger stage. On the other hand it is expected that the front-end electronics will be developed in a smaller feature size

process, such as $0.13\ \mu\text{m}$ CMOS. For this process and a sensor capacitance of 5 pF (current strip sensor capacitances range from 10-25 pF) a decrease of the front-end power per channel by roughly a factor of 5 was estimated [3], an advantage that is partly canceled by lowering the operating voltage from 2.5 V to 1.2-1.3 V. In total, while the power consumption of the upgrade tracker is not precisely known as of today, it is very likely that it will equal or exceed the current power consumption. While an increase of the number or cross-section of cables is not desirable due to the expected increase of the material budget and the accompanying negative effect on the detector performance, it is even considered practically impossible since the tracker services are buried beneath the services of the electromagnetic calorimeter, and since the space available in the service channels is already occupied by the current services.

B. DC-DC Conversion

To deal with the problem, which affects both the ATLAS and CMS trackers, two solutions have been proposed: Serial Powering (SP) and powering with DC-DC converters. While in SP a number of modules are connected in series to a constant current source, DC-DC converters [4] are used to convert a high DC input voltage to a lower DC output voltage. In this paper, we concentrate on the latter option.

The ratio of the output to the input voltage, V_{out}/V_{in} , is called the conversion ratio, here denoted as r . If r is small, ideally much smaller than 1, the input current can be smaller by the same factor, leading to a reduction of the power loss by r^2 . In a simple approach, one converter could be installed per module. Several technologies exist, but mostly inductors or capacitors are used as energy storage elements. For each technology there is a great variety of topologies and designs. The simplest inductor-based step-down (i.e. $r < 1$) converter type is the “buck” converter. Its basic circuit consists of a switch, which is typically implemented as two transistors, an inductor for energy storage, and a filter capacitor. Realistic devices feature also a feedback circuit based on Pulse Width Modulation (PWM). DC-DC converters are flexible: with the same basic circuit, various output voltages can be achieved with minor re-configurations, and several converter stages can be combined. In contrast to capacitor-based approaches, inductor-based designs can in general provide currents of several Amperes. Challenges are the achievement of an efficiency as high as possible, the need for a radiation-hard technology that supports the high input voltage (expected to be around 10 V for SLHC applications), as well as the potential generation of switching noise. Another issue for inductor-based layouts is the requirement to operate in a high

magnetic field (4 T for CMS): since ferrite materials saturate, air-core inductors must be used. To achieve the necessary inductances, these coils must be relatively large and massive. Due to the far extension of the magnetic field, the radiation of electromagnetic noise is a potential issue.

To understand better the opportunities and challenges related to this proposed solution to the power problem, we have performed system test measurements with commercial and custom DC-DC converters.

II. THE SYSTEM TEST

A. Set-up Description

In the absence of any prototype structures for the tracker upgrade, substructures of the current tracker end caps, referred to as petals, have been used. While future devices will be different in many respects, we believe that lessons can be learned from operating current tracker structures with DC-DC converters.

The petals as well as the data acquisition chain are described elsewhere [1]. Here only aspects of the front-end (FE) electronics relevant for the system test are described. The test petal was equipped with four ring-6 modules. This module type carries two daisy-chained sensors with AC-coupled p-doped strips implanted in a 500 μm thick n-doped bulk. The sensor capacitance amounts to about 20 pF. The connections between sensors and between the first sensor and the FE-electronics are realized with wire bonds. The FE-hybrid carries six APV25 readout chips [5], which are manufactured in a 0.25 μm CMOS process. Each chip processes the data of 128 channels. The read-out is fully analogue. For each channel, a charge-sensitive pre-amplifier, a CR-RC filter with a time constant of 50 ns, and a 192 cells deep pipeline are implemented. The data are sampled at 40 MHz. Two readout modes can be selected: in peak mode only one sample is used per event; in deconvolution mode a weighted sum of three consecutive samples is formed to reduce the effective shaping time to 25 ns. On receipt of a level-1 trigger, the data are output with a rate of 20 MS/s. Data of two APVs are multiplexed onto one optical channel by the APVMUX chip, resulting in a 40 MS/s serial output stream. The APV25 is powered from two supply rails, namely 1.25 V and 2.5 V. Typical currents are 60 mA and 120 mA, respectively [2]. All other chips on the hybrid as well as the analog-optical converters (Analog-Opto Hybrids, AOH) and the controller chips (Central Control Units, CCU) operate with a supply voltage of 2.5 V.

All modules have been powered and read-out during the measurements. The petal was equipped with the original motherboards (InterConnect Board, ICB), AOHs and CCU modules. Both readout and digital signalling (trigger, clock, fast controls) was realized optically. PCI-based prototypes of the ADC card (Front End Driver), the trigger card (Trigger Sequencer Card) and the controller card (Front End Controller) have been used. The petal has been thermally stabilized at +15 °C. It was housed in a grounded metal box. The set-up was very similar to test systems used during integration of the CMS tracker [6].

The modules have been commissioned with a well-known procedure and operated with fully depleted sensors, mostly in peak mode.

B. Analysis Method

The analysis method is described in [6]. The raw or total noise is calculated as the RMS of the fluctuations around the pedestal value, which is the mean strip signal without particles traversing the detector. The common mode (CM) is defined as a common event-wise fluctuation of all strips of an APV, and is calculated as the median of the signals after subtraction of the pedestals. It is included in the raw noise. The common mode noise is the RMS of the common mode. At least 100 000 events have been taken per run to assure stable conditions, of which 10 000 events, starting from event 90 000, have been analyzed.

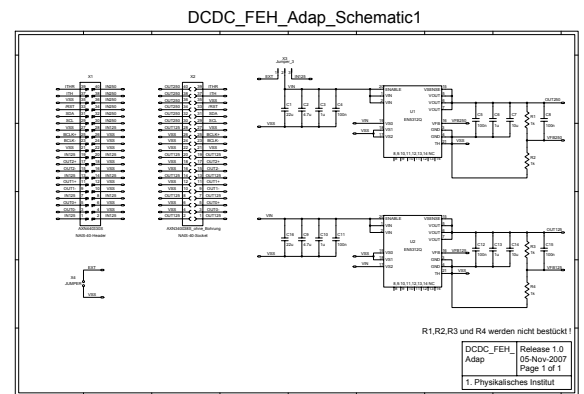
III. MEASUREMENT RESULTS

A. Commercial DC-DC Converters with Internal Ferrite Inductors

Since custom radiation-hard DC-DC converters were not available when we started our investigations, we used commercial buck converters. The first tests were performed with buck converters with internal coils.

A market survey was performed to identify a device with high switching frequency (i.e. small size of passive components), low conversion ratio, a suitable output voltage range and sufficient output current. The Enpirion buck converter EN5312QI [7] was chosen: with dimensions of 5x4x1.1 mm³, a switching frequency of 4 MHz and a maximum current of 1 A it is appropriate for our application. A disadvantage is the relatively low recommended maximal input voltage of 5.5 V. The device implements an internal planar inductor in MEMS technology. Due to the deployment of magnetic cores it is not usable in a strong magnetic field.

Two such devices, configured to provide 2.5 V and 1.25 V, respectively, were mounted on a four-layer PCB, together with input and output filter capacitors and connectors (Figs. 1 and 2). This PCB can be plugged between the ICB and the module. Two versions of the PCB have been tested: the L type (Fig. 2, left) is slightly larger, the S type (Fig. 2, right) is smaller and more modular in design (separate PCB for connector).



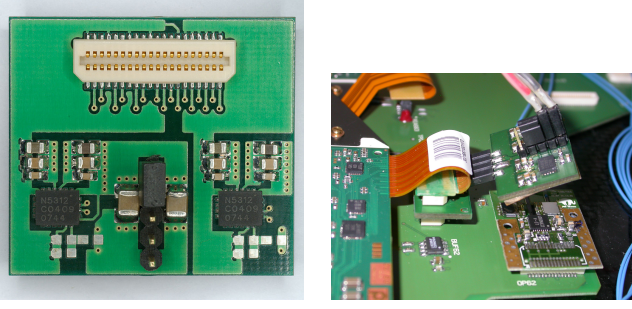


Figure 2: The converter PCBs: L type (left) and S type integrated onto the petal (right).

The input power is supplied either directly from an external power supply (PS), or via the 1.25 V plane of the ICB. No difference in performance was observed between these options. In most measurements, the board was powered with 5.5 V directly from an Agilent E3633A PS.

The raw noise distribution of one module is shown in Fig. 3 (the results for other modules are similar and not shown here). The noise level is slightly increased by up to 10% (note the zero-suppression on the y-axis). The additional contribution is common mode, as reflected e.g. in a broadening of the CM distribution. With the S type board, the increase of noise is almost negligible. The difference between the boards has been traced back to the additional connection between the main and “connector PCB”. Clearly a careful PCB design is very important to achieve an optimal noise performance. Further studies have mostly been performed with L type boards.

Edge strip channels are known to be sensitive to noise effects, such as coupling from the bias ring or common mode due to bad grounding. With converters, the noise on module edge strips increases by up to a factor of 10 (Fig. 4). Furthermore, the noise on disconnected channels increased from a low level to a level even above the mean. For the interpretation the common mode subtraction inside the APV has to be considered [8]. Each APV channel implements an inverter stage. These are powered from 2.5 V via a common resistor, located on the FE-hybrid. If a common mode signal is present at the inputs of the inverters, a voltage drop is created across the resistor that drives down the inverter output and effectively subtracts the common mode from it. This, however, does not apply to channels which see a lower than normal CM, such as disconnected channels, or a higher than normal CM, such as edge channels. If a certain common mode is present in the system, the CM they see will be over-compensated or not completely subtracted, respectively. Their signal is thus a sensitive indicator of the CM actually present in the system. Further studies have shown that connecting the converters only to 1.25 V, used to power the pre-amplifier, does not lead to any increase of CM on normal strips, while connecting converters only to 2.5 V, used in all other stages of the chip, does increase the noise. The edge strip noise is increased in both cases. The current understanding is that noise coupled in before the inverter can effectively be subtracted, except on edge strips and bad channels. Noise coupled in after the inverter, i.e. via 2.5 V, cannot be subtracted and is visible.

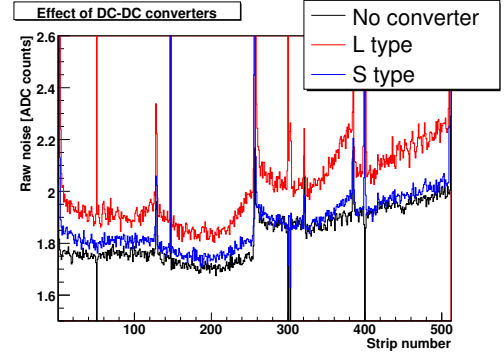


Figure 3: Raw noise for conventional powering (black) and powering via L type (red) and S type (blue) DC-DC converter PCBs.

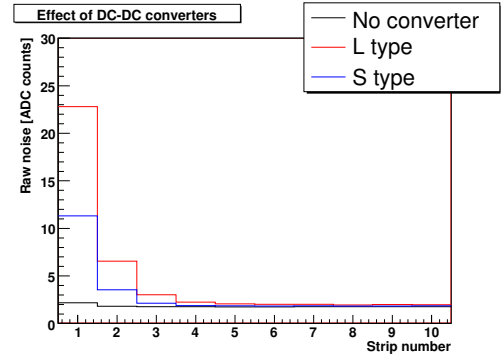


Figure 4: Edge strip noise for conventional powering (black) and powering via L type (red) and S type (blue) DC-DC converter PCBs.

To study potential cross-talk effects, the correlation matrix between all pairs of strips has been computed for two adjacent modules that were powered with converters. The correlation coefficients are defined as $corr_{ij} = (\langle r_i \cdot r_j \rangle - \langle r_i \rangle \langle r_j \rangle) / (\sigma_i \cdot \sigma_j)$, where r_i and σ_i are the raw data and noise of strip i , respectively. With ordinary powering, correlations amount to around 5% both for strip pairs within and between modules. With converters, correlations of 10-20% are observed for strip pairs within modules, reflecting the increased common mode. The correlations between modules are however not increased significantly, i.e. cross-talk between modules is not observed.

To investigate the potential effect of a Low DropOut regulator (LDO) on the voltage ripple and thus the noise, another PCB was developed. The LDO LTC3026 from Linear Technology [9] was connected to the output of EN5312QI. A ripple rejection of around 45 dB for the switching frequency of 4 MHz is quoted in the data sheet. Tests were performed with dropouts of 50 and 100 mV. As visible in Fig. 5 for a dropout of 50 mV, a beneficial effect is observed: the raw noise is no more increased and the noise on edge strips is “only” a factor of 2 above the normal level. We conclude that the noise in our system is mainly caused by a conductive coupling of a differential mode component of the converter noise.

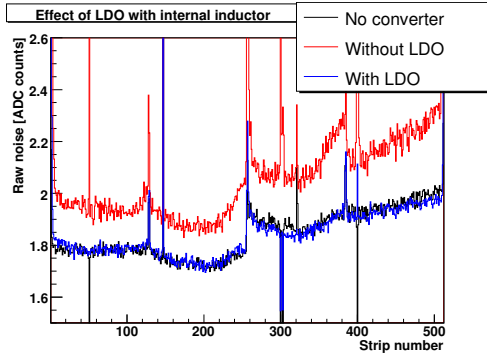


Figure 5: Raw noise for conventional powering (black) and powering with a L type PCB with (blue) and without (red) LDO.

B. Commercial DC-DC Converters with External Air-Core Inductors

Since ferrite inductors cannot be used in the final experiment, commercial buck converters have been equipped with external air-core inductors. For these tests, the Enpirion buck converter EQ5382D has been chosen, which is similar to EN5312QI, but has no internal inductor. PCBs similar to the L type have been fabricated and equipped with various coils: planar ferrite inductors (Murata LQH32CN1R0M23, $L = 1 \mu\text{H}$), air-core solenoids (Coilcraft 132-20SMJLB, $L = 538 \text{ nH}$) and custom-made air-core toroids ($L \approx 600 \text{ nH}$). With air-core inductors, the noise increases drastically compared to internal or external ferrite inductors (Fig. 6). For toroids the increase is a factor of 2-3 lower than with solenoids. The edge strip noise increases enormously, up to about 90 ADC counts. When a module was operated with an air-core coil, the noise increased also on its conventionally powered neighbour modules.

The wing-shaped noise has been traced to a pick-up of radiated noise in the FE-hybrid region. This has been proven in tests where the module was powered conventionally but exposed to the radiation of noise by powered but unplugged converter boards or individual coils operated with a frequency generator. In both cases, wing-shaped noise was induced in the module. In one test the PCB was placed above the conventionally powered module and the position of the converter board was varied systematically. For each position the mean module noise was computed. The biggest effect was observed when the PCB was placed above the FE-hybrid, while the effect was very small when the board was located above the sensor. With air-core coils the conductively generated noise is increased as well, presumably by noise coupling from the coil into the PCB itself. Further studies are needed to understand the details of the coupling mechanisms and the shapes of the distributions. As expected, using a LDO does decrease the conductive part, but not the wings (Fig. 6).

Tests have been performed with shielded converters. The PCB was wrapped in copper or aluminium foil of 35 and $30 \mu\text{m}$ thickness, respectively. The noise decreased significantly (Fig. 7). Grounding the shield did not improve the situation. No further improvement was obtained with thicker shields.

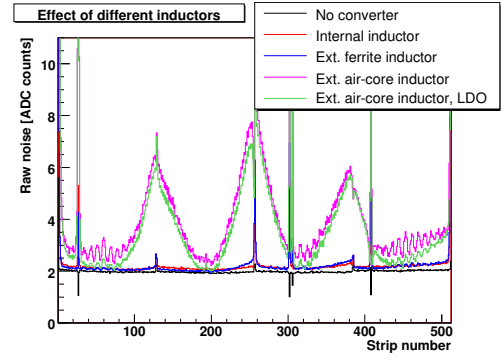


Figure 6: Raw noise for conventional powering (black) and powering with a L type PCB with internal coil (blue), external ferrite coil (red) and external air-core solenoid without (pink) and with (green) LDO.

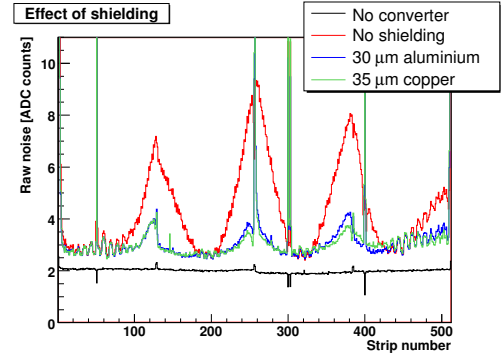


Figure 7: Raw noise for conventional powering (black) and powering with a L type PCB with external air-core solenoid, without shielding (red) and with $35 \mu\text{m}$ copper (green) or $30 \mu\text{m}$ aluminium shielding (blue).

The chosen foils might already be thicker than necessary and thinner shields should be tried. The noise contribution remaining with shielding is probably induced conductively. While shielding is in general not desirable due to the associated material, adding an aluminium box of $(3 \text{ cm})^3$ (a very conservative assumption) and a thickness of $30 \mu\text{m}$ for instance to each module in the end caps would increase their mass by only 1.5 kg (2 per mille).

Finally the distance between the converter PCB and the FE-hybrid has been varied. For this test, the L type board with external air-core solenoids has been equipped with an S type connector. A cable has been plugged between the board and the “connector PCB”, so that distance and cable length could be varied. The noise effect depends strongly on the distance. When the distance is increased by a few centimetres, the increase of noise is almost negligible. It should be noted that the conductive noise is decreased as well due to passive filtering in the connector and cable. While space around single modules is expected to be very constraint in a new tracker, an operation of buck converters on the substructure level could thus be feasible.

C. Custom DC-DC Converters

1. The SWREG2 Buck PWM Controller (CERN)

A single phase buck PWM Controller with Integrated MOSFET is being developed at CERN [10]. The first prototype chip (SWREG2) in AMIS I3T80 technology became available shortly before the conference. The chip accepts input voltages from 3.3-20 V; the maximum output current is 2 A. The SWREG2 implements the transistors and the logic of the feedback control circuit. Together with external components like voltage references, filter and bootstrap capacitors and of course the air-core coil it is mounted on a 4-layer PCB (RWTH Aachen). The output voltage is configurable via a resistor. A tunable saw-tooth signal for the PWM is provided from a separate PCB and thus the switching frequency can be varied between 250 kHz and 3 MHz.

During the test the SWREG2 provided the 2.5 V for the FE-hybrid, while the 1.25 V was supplied by an external PS. The distance of the board to the FE-hybrid amounted to several centimetres, so that the effect from conductive noise could be isolated. Data have been recorded for an input voltage of 5.5 V and several switching frequencies between 0.6 and 1.25 MHz (Fig. 8). Independently of the frequency, the noise level is increased by about 20%, and a noise ripple with a period of eight strips is observed. When the data are plotted in the order which is realized after the multiplexing stage of the APV, the ripple is eliminated and the noise varies smoothly with the sample number. This indicates that the noise couples into the back-end stages of the APV, i.e. in the stages after the multiplexer. This phenomenon has not been observed with any commercial converter.

2. Charge Pump (LBNL)

DC-DC converters that utilize capacitors instead of inductors as energy storage elements are commonly referred to as charge pumps. For a step-down converter, a number of capacitors are charged in series during the first phase and discharged in parallel during the second phase of the switching cycle. The output current is equal to the input current times the number of parallel capacitors.

A charge pump with divide-by-four stack configuration with three “flying” capacitors has been developed at LBNL [11]. The PCB implements a $0.35\ \mu\text{m}$ CMOS IC with switches and driver circuits plus $1\ \mu\text{F}$ input and flying capacitors and a $10\ \mu\text{F}$ output capacitor. The switching frequency is 0.5 MHz. Due to the relatively small output current of 0.5 A, two charge pumps are connected in parallel on one “tandem” converter board. The capacitors of the two charge pumps charge either in-phase or with alternating phase. In the latter case, a lower output current ripple is expected. The PCBs have been used to power either 1.25 V or 2.5 V, while the second voltage was provided by an external PS. With the alt-phase PCB providing 2.5 V, the noise increases by about 20%, similar to the SWREG2, while the in-phase version leads to an increase by about 75%. When the converter was used to deliver the 1.25 V, only the noise on edge channels increased, in agreement with observations with the EN5312QL.

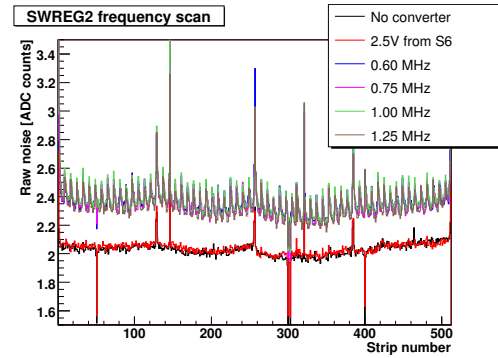


Figure 8: Raw noise for conventional powering (black), powering the 2.5 V with a S type PCB (red) or with the SWREG2 buck converter with a switching frequency of 0.6 MHz (blue), 0.75 MHz (pink), 1.0 MHz (green) and 1.25 MHz (brown).

IV. SUMMARY

Commercial buck converters with internal and external inductors as well as custom prototypes of a buck converter and a charge pump have been tested with CMS silicon strip modules. An increase of the noise level and the module edge strip noise due to the ripple and switching noise on the converter output voltage has been measured consistently in all cases. In addition, pick-up of noise radiated from air-core inductors was observed. Several countermeasures have been studied: implementation of a LDO, shielding, variation of the distance etc. While operation of buck converters close to individual modules seems to be disfavoured due to noise and space constraints, the operation of buck converters at substructure level in a 2-step approach could be possible. More studies are however needed to understand better the noise coupling mechanisms and to proof the viability of a power distribution scheme based on DC-DC converters.

REFERENCES

- [1] The CMS Collaboration, JINST **3** S08004M (2008).
- [2] S. Paoletti, TWEPP 2007, CERN-2007-007 (2007).
- [3] M. Raymond, these proceedings.
- [4] R. W. Erickson, *DC-DC Power Converters*, Wiley Encyclopedia of Electrical and Electronics Engineering (2007).
- [5] M. Raymond et al., LEB 2000, CERN-2000-010 (2000).
- [6] R. Bremer, PhD Thesis, CMS TS-2008/012 (2008).
- [7] Enpirion, USA; <http://www.enpirion.com/>
- [8] M. Raymond, [http://icva.hep.ph.ic.ac.uk/~dmray/ ...pptfiles/CMStracker31_10_01.ppt](http://icva.hep.ph.ic.ac.uk/~dmray/...pptfiles/CMStracker31_10_01.ppt).
- [9] Linear Technology, USA; <http://www.linear.com/>
- [10] S. Michelis et al., TWEPP 2007, CERN-2007-007 (2007); and these proceedings.
- [11] P. Denes et al., *A Capacitor Charge Pump DC-DC Converter for Physics Instrumentation*, submitted to IEEE Transactions on Nuclear Science (2008).